Modeling the Thermodynamic and Transport Properties of Decahydronaphthalene/Propane Mixtures: Phase Equilibria, Density, and Viscosity

Nathaniel Cain[1], George Roberts[1], Douglas Kiserow[1, 2], Ruben Carbonell[1]

[1]North Carolina State University, Department of Chemical & Biomolecular Engineering, 1017 Main Campus Drive, Partners' Building I, Suite 3200, Box 7006, Raleigh, NC 27606-7006

Phone: 919-515-5118, Fax: 919-515-5831; contact e-mail: ruben@ncsu.edu

[2]U.S. Army Research Office, 4300 So. Miami Blvd, Research Triangle Park, NC, 27709

Abstract

The density and viscosity of propane mixed with 66/34 *trans/cis*-decahydronaphthalene were measured over a wide range of temperatures (323 – 423K), pressures (2.5-208 bar), and compositions (0-65 mol% propane). For conditions giving two phases, the composition of the dense phase was measured in addition to the density and viscosity. The modified Sanchez-Lacombe equation of state (MSLEOS) was used with a single linearly temperature-dependent pseudo-binary interaction parameter to correlate the phase compositions and densities. The compositions and densities of the mixtures were captured well with absolute average deviations between the model and the data of 5.3% and 2.3%, respectively. The mixture viscosities were computed from a free volume model (FVM) by using a single constant binary interaction parameter. Density predictions from the MSLEOS were used as input mixture density values required for the FVM. The FVM was found to correlate well with the mixture viscosity data with an absolute average deviation between the model and the data of 5.7%.

Report Documentation Page		*Form Approved* *OMB No. 0704-0188*

Public reporting burden for the collection of information is estimated to average 1 hour per response, including the time for reviewing instructions, searching existing data sources, gathering and maintaining the data needed, and completing and reviewing the collection of information. Send comments regarding this burden estimate or any other aspect of this collection of information, including suggestions for reducing this burden, to Washington Headquarters Services, Directorate for Information Operations and Reports, 1215 Jefferson Davis Highway, Suite 1204, Arlington VA 22202-4302. Respondents should be aware that notwithstanding any other provision of law, no person shall be subject to a penalty for failing to comply with a collection of information if it does not display a currently valid OMB control number.

1. REPORT DATE **2011**	2. REPORT TYPE	3. DATES COVERED **00-00-2011 to 00-00-2011**
4. TITLE AND SUBTITLE **Modeling The Thermodynamic And Transport Properties Of Decahydronaphthalene/Propane Mixtures: Phase Equilibria, Density, And Viscosity**		5a. CONTRACT NUMBER
		5b. GRANT NUMBER
		5c. PROGRAM ELEMENT NUMBER
6. AUTHOR(S)		5d. PROJECT NUMBER
		5e. TASK NUMBER
		5f. WORK UNIT NUMBER
7. PERFORMING ORGANIZATION NAME(S) AND ADDRESS(ES) **U.S. Army Research Office,4300 So. Miami Blvd,Research Triangle Park,NC,27709**		8. PERFORMING ORGANIZATION REPORT NUMBER
9. SPONSORING/MONITORING AGENCY NAME(S) AND ADDRESS(ES)		10. SPONSOR/MONITOR'S ACRONYM(S)
		11. SPONSOR/MONITOR'S REPORT NUMBER(S)

12. DISTRIBUTION/AVAILABILITY STATEMENT **Approved for public release; distribution unlimited**

13. SUPPLEMENTARY NOTES

14. ABSTRACT

The density and viscosity of propane mixed with 66/34 trans/cis-decahydronaphthalene were measured over a wide range of temperatures (323 ? 423K), pressures (2.5-208 bar), and compositions (0-65 mol% propane). For conditions giving two phases, the composition of the dense phase was measured in addition to the density and viscosity. The modified Sanchez-Lacombe equation of state (MSLEOS) was used with a single linearly temperature-dependent pseudo-binary interaction parameter to correlate the phase compositions and densities. The compositions and densities of the mixtures were captured well with absolute average deviations between the model and the data of 5.3% and 2.3%, respectively. The mixture viscosities were computed from a free volume model (FVM) by using a single constant binary interaction parameter. Density predictions from the MSLEOS were used as input mixture density values required for the FVM. The FVM was found to correlate well with the mixture viscosity data with an absolute average deviation between the model and the data of 5.7%.

15. SUBJECT TERMS					
16. SECURITY CLASSIFICATION OF:			17. LIMITATION OF ABSTRACT	18. NUMBER OF PAGES	19a. NAME OF RESPONSIBLE PERSON
a. REPORT **unclassified**	b. ABSTRACT **unclassified**	c. THIS PAGE **unclassified**	**Same as Report (SAR)**	**35**	

1. Introduction

Organic solvents expanded with supercritical fluids (ScF) have been investigated as alternative chemical process media for more than two decades. ScF expanded liquids can provide an otherwise difficult-to-achieve range of solute solubilities obtained by mixing a good solvent (the organic liquid) with a poor solvent (the ScF). Recently, ScF/solvent combinations have been recognized as unique and, in some cases, beneficial chemical reaction solvents [1]. For mass transfer-controlled reactions, the addition of a ScF can improve reaction rates by increasing mass transfer rates in the fluid phase and to the internal surfaces of porous catalysts. As examples, solvents expanded by supercritical and subcritical ScFs have been used in homogeneous catalytic oxidations [2], heterogeneous catalytic oxidations [3], and heterogeneous hydrogenations {4-7}.

The addition of a ScF to polymer/organic solvent solutions has been investigated extensively as a technique to decrease the lower critical solution temperature (LCST) allowing a less aggressively attainable phase split for polymer separation/purification [8-14]. Recently, the hydrogenation of polystyrene (PS) has been investigated in decahydronaphthalene (DHN) expanded by supercritical carbon dioxide (scCO$_2$) [4, 5, 7]. Although the addition of scCO$_2$ improved the hydrogenation rate under many circumstances, unwanted carbon monoxide (CO) was produced via the reverse water gas shift reaction (RWGSR). When the concurrent

production of CO is unavoidable, methanation metals like Ni or Ru can be used to mitigate CO poisoning of the hydrogenation catalyst [4, 7].

Alternatively, propane (C3) can, in principle, replace CO_2 in this reaction to eliminate the formation of CO entirely. The results presented here are germane to that alternative for PS hydrogenation. Due to the high cost of the pure isomers of DHN, a commercial mixture of *trans/cis*-DHN produced by DuPont (Decalin®) was used for our studies. The composition of commercially available DHN samples ranges from almost 100% *trans*-DHN to an isomeric mixture with as little as 40% *trans*-DHN [15]. Polystyrene phase separation behavior in DHN has been reported and has been interpreted in light of the properties of the solvent [16]. For C3 expanded DHN, fundamental thermophysical data are lacking in the literature and thermophysical data for PS in C3/DHN mixtures have not been published. In this paper, we report thermophysical data for mixtures of DHN and C3. We use the modified Sanchez-Lacombe Equation of State (MSLEOS) to fit phase density and composition data and a free volume model (FVM) to fit the mixture viscosity data. This data is of significant importance in analyzing the performance of PS hydrogenation reactions in high-pressure C3/DHN mixtures.

2.   Materials and Methods

Research grade C3 (99.99%, Airgas National Welders) and high purity 66/34 wt% *trans/cis*-DHN (99+%, Sigma-Aldrich) were used for all measurements. All chemicals were used as-received. The phase behavior and densities of C3/DHN mixtures were measured in a variable-volume view cell housed within a thermostatted ($\pm$ 0.2 $^{\circ}$C) oven. A schematic diagram of the experimental apparatus is shown in Figure 1. Pressure was transmitted from the sample fluid through a chemical seal (L990.34, WIKA Instrument Corp.) to a pressure transducer (PX309-10KGV, Omegadyne, $\pm$ 1.7 bar) mounted outside of the oven. Silicon oil

(Phenylmethyl Siloxane, Dow Corning) was used as the pressure transmitting fluid. Linear displacement of the piston was measured using a micrometer (CD-6"CSX, Mitutoyo). A calibration curve of volume versus displacement was made by adding a known amount of CO_2 and measuring the displacement of the piston at temperatures and pressures where the densities were known. Pure component and mixture densities were measured using the calibration curve along with the mass of the sample loaded into the view cell. All wetted surfaces were Teflon™ or 316 stainless steel.
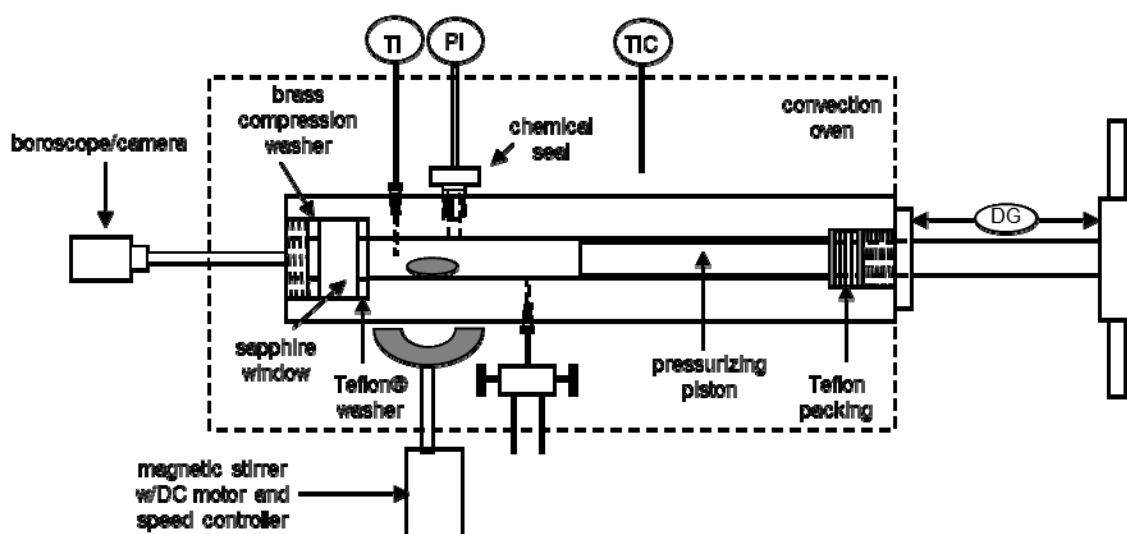

Figure 1 Schematic of phase equilibria apparatus [TI: temperature indicator, PI: pressure indicator, TIC: temperature indicator/controller, DG: displacement gauge]

Viscosities were measured using a SPL440 high-pressure viscometer (Cambridge Applied Systems, Cambridge, MA) equipped with a variable-volume view cell and an external recirculation pump (Micropump GAH.X21, Idex, Oak Harbor, WA) used for mixing. A schematic of the experimental apparatus is shown in Figure 2. The external gear pump head was rapped with insulation to minimize heat losses during recirculation. The pressure was maintained well above a predetermined pressure to ensure a single fluid phase. The mixture was assumed homogeneous when convergence of the measured viscosity was obtained after checking

the viscosity at different intervals during recirculation. Once the mixture was assumed homogeneous the 2-way and 3-way valves were closed to the recirculation loop to isolate the measurement fluid in the oven from the fluid outside the oven in the recirculation pump. Precautions were taken to ensure phase separation did not occur between measurements at a given composition. The viscosity of the fluid is measured by recording the time it takes the piston to move between the two magnetic coils. This time is converted to a value of viscosity in centipoise (cP) by an internal calibration supplied by the manufacturer. Before each viscometer experiment the viscometer apparatus was leak checked by charging with carbon dioxide and pressurizing to 346 bar. The viscometer was evacuated and charged with propane three times to remove residual carbon dioxide. For an actual viscosity experiment, C3 was charged to the cell with a high pressure syringe pump (500D, Teledyne Isco). The mass of C3 added to the view cell was computed from the change in volume of the syringe pump at the temperature and pressure of the syringe pump using the known densities of C3. A sample bomb was used to measure the accuracy of the C3 addition procedure. The difference between the calculated mass from the syringe pump and gravimetrically measured mass added to the sample bomb was at most 0.1%. The estimated standard uncertainties for temperature, pressure, and C3 mole fraction were 0.05 K, 0.06 bar, and 0.005 mole C3/mol, respectively. The estimated combined expanded uncertainty for viscosity and density were 0.027 cP, and 0.002 g/cm^3, respectively.
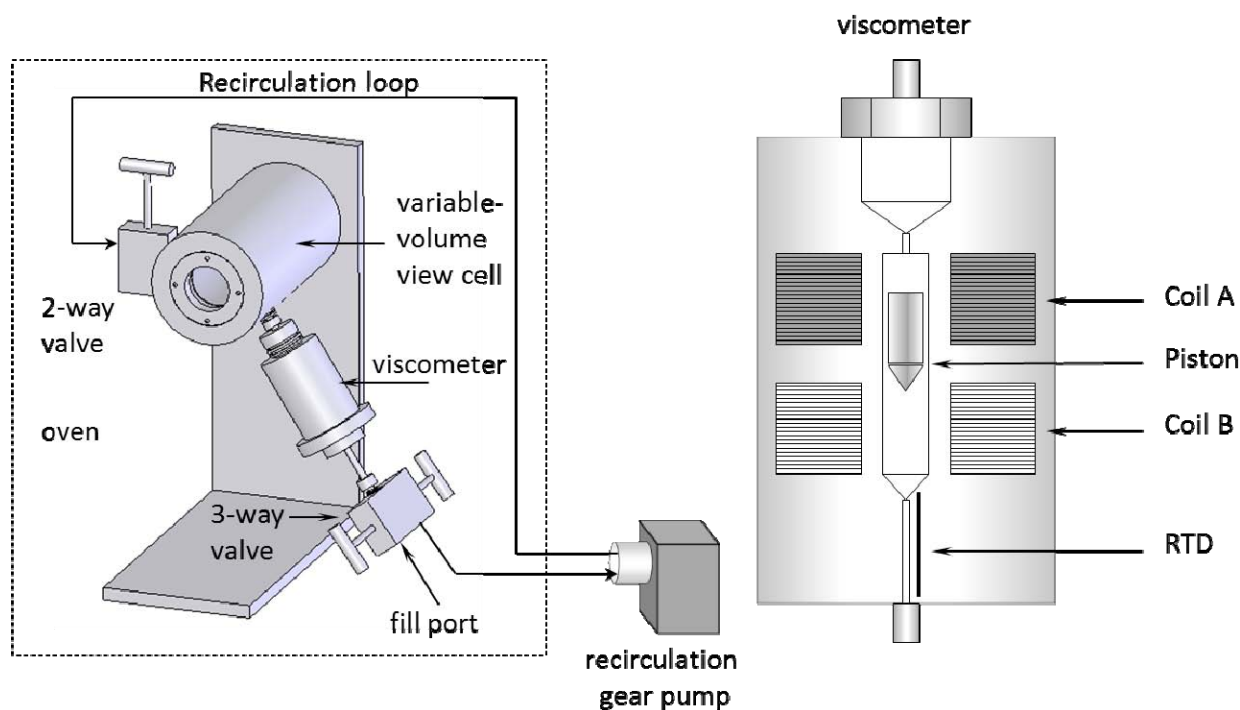
Figure 2   Schematic of high pressure viscometer experimental apparatus

The saturated liquid density and vapor pressure of C3 are well established [17, 18]. Therefore, we used C3 to validate the operation of the view cell for vapor pressure and density measurements. The measured vapor pressures are compared to literature values in Figure 3. The vapor pressure was measured by recording the pressure when the first bubble appeared during a decompression experiment. The process was repeated several times to ensure reproducibility. The vapor pressure was also measured by recording the pressure when the cell was approximately 50% liquid and 50% vapor and was allowed to equilibrate for approximately one hour. There was negligible difference between the two methods so we have not separated values accordingly in Figure 3. Volumes were measured by precision micrometry as described previously in the text. Saturated liquid densities of C3 were measured at the bubble point and are plotted in Figure 4.
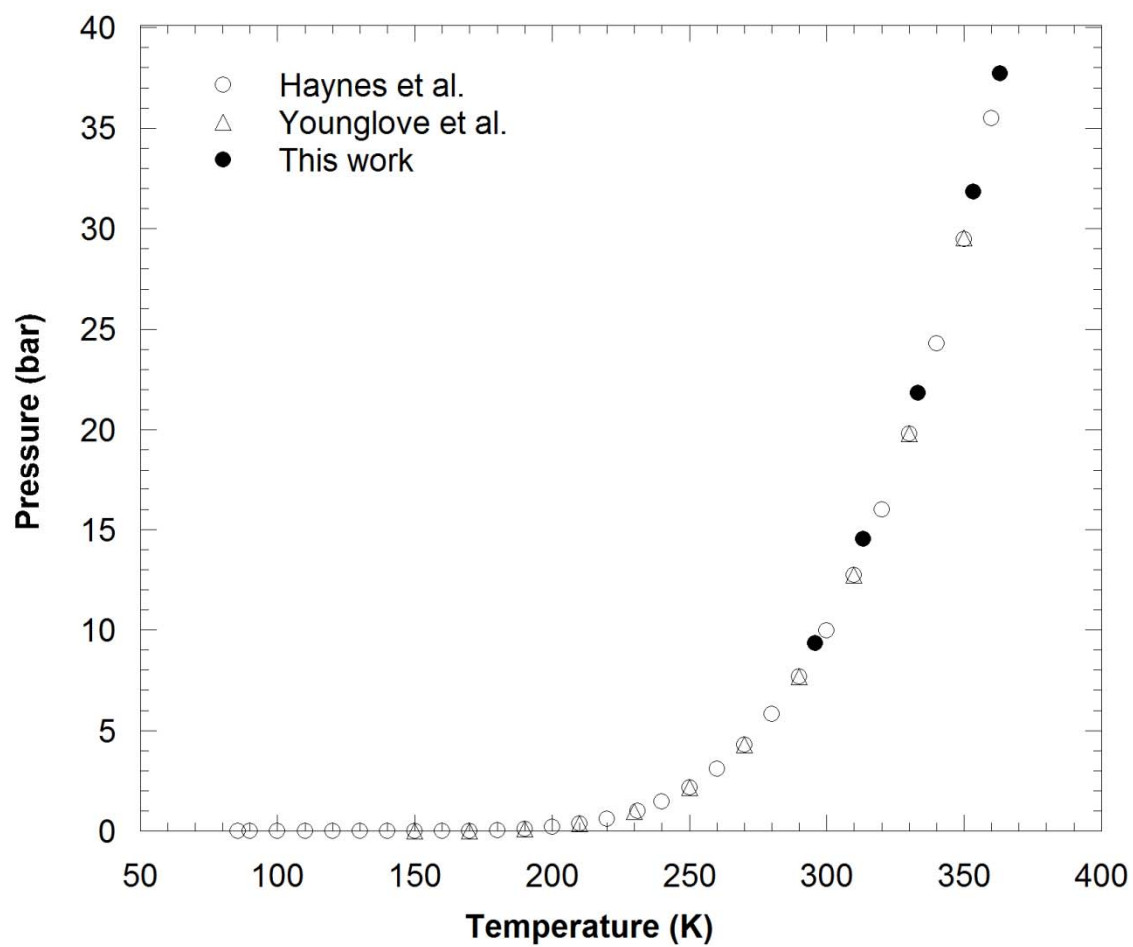
Figure 3   Comparison of measured and reported C3 saturated vapor pressure data
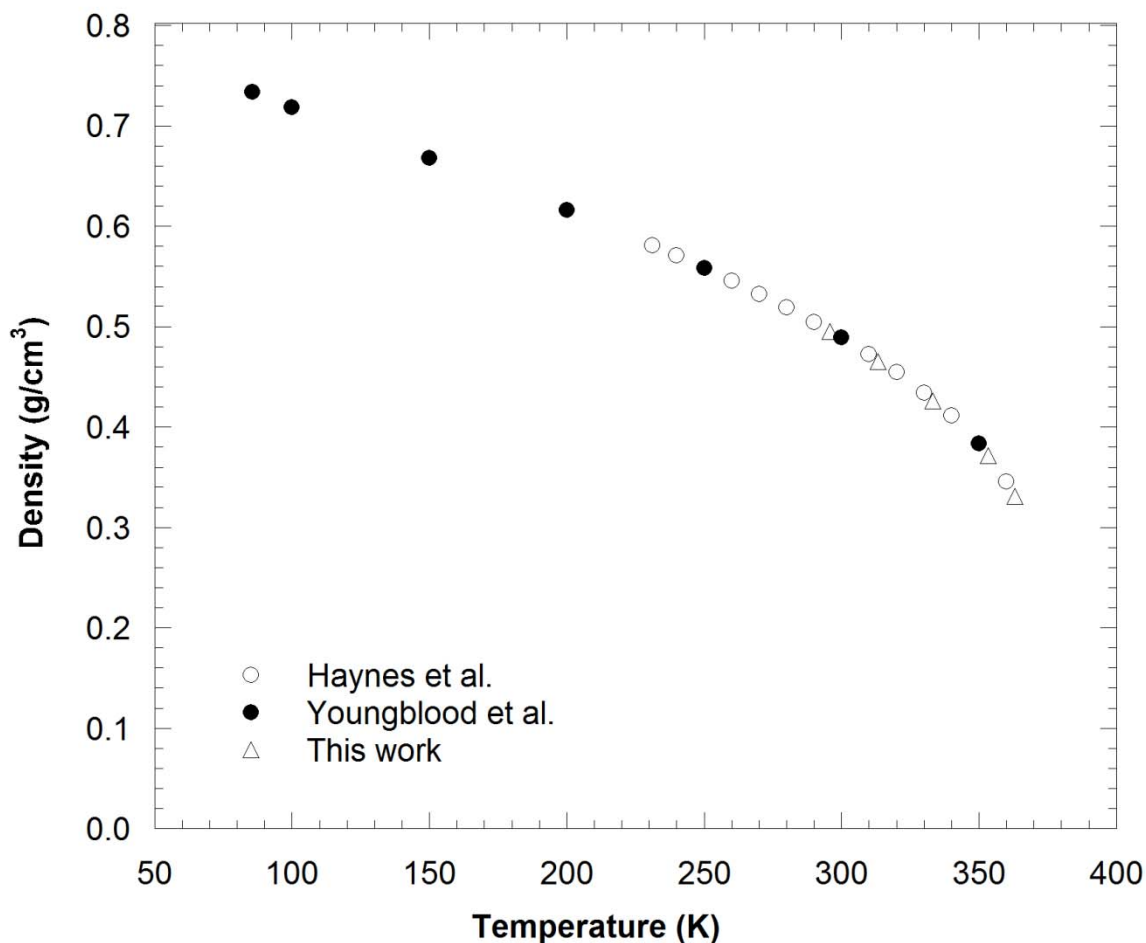
Figure 4   Comparison of measured and reported C3 saturated liquid density data

3.   Phase equilibria and density model

The lattice-fluid model proposed by Sanchez and Lacombe [19, 20, 21], expresses the reduced density as a function of the reduced temperature and the reduced pressure (Equation 1). Their EOS has been used to describe the thermodynamic properties of many complex systems, including organic liquid/ScF mixtures [22], polymer/organic liquid solutions [16, 23], and polymer/organic liquid/ScF solutions [14, 24].   The Sanchez-Lacombe equation-of-state (SLEOS) uses three pure component parameters to characterize the phase behavior. Typically, the parameters are obtained by fitting the EOS to pure component saturated vapor pressure data [20],

$$\tilde{P} = -\tilde{T}\left[\ln\left(1-\tilde{\rho}\right) + \left(1-\frac{1}{r}\right)\tilde{\rho}\right] - \tilde{\rho}^2 \tag{1}$$

The reduced properties are defined as:

$$\tilde{P} = \frac{P}{P^*} = \frac{P\upsilon^*}{\varepsilon^*} \qquad \tilde{T} = \frac{T}{T^*} = \frac{RT}{\varepsilon^*} \qquad \tilde{\rho} = \frac{1}{\tilde{\upsilon}} = \frac{\rho}{\rho^*} = \frac{r\upsilon^*}{\upsilon} \tag{2}$$

Neau showed that the SLEOS can give thermodynamically inconsistent phase equilibria predictions. This occurs when the SLEOS is combined with certain commonly used mixing rules. In particular, inconsistent results are obtained when mixing rules are computed using literature chemical potentials derived on the basis of the Helmholtz energy obtained from the partition function of mixtures [22]. More specifically, the reference chemical potential at the ideal gas state leads to compositional dependence for commonly used mixture rules and hence is thermodynamically inconsistent. Neau suggested instead the use of fugacity coefficients derived from the SLEOS. Her approach gives thermodynamically consistent phase equilibria predictions and her results correlate better to binary data for CO_2/n-hexane than did predictions using literature chemical potentials with the same mixing rules.

Following Neau, fugacity coefficients are calculated from the expression [23],

$$\ln\varphi_i\left(T,P,x_j\right) = -\ln z + r_i\left[-2\frac{\tilde{\rho}}{\tilde{T}} - \ln\left(1-\tilde{\rho}\right)\right]$$
$$+\left(\frac{z-1}{r}\right)\left[\frac{nr}{\upsilon^*}\left(\frac{\partial\upsilon^*}{\partial n_i}\right)_{n_j}\right] - \frac{\tilde{\rho}}{\tilde{T}}\left[\frac{nr}{\varepsilon^*}\left(\frac{\partial\varepsilon^*}{\partial n_i}\right)_{n_j}\right] \quad (i=1,...,c) \tag{3}$$

The corresponding compressibility factor z is calculated from the EOS via the equation,

$$z = \frac{P\upsilon}{RT} = \frac{\tilde{P}\tilde{\upsilon}}{\tilde{T}}r = r\left[-\frac{1}{\tilde{\rho}}\ln\left(1-\tilde{\rho}\right) - \left(1-\frac{1}{r}\right) - \frac{\tilde{\rho}}{\tilde{T}}\right] \tag{4}$$

The commonly used "k_{ij}, l_{ij}" mixing rules given by McHugh and Krukonis [25] were used in our work and are defined as follows:

$$\upsilon^* = \sum\sum\phi_i\phi_j\upsilon_{ij}^*, \qquad \upsilon_{ij}^* = \frac{1}{2}\left(\upsilon_{ii}^* + \upsilon_{jj}^*\right)\left(1 - l_{ij}\right) \tag{5}$$

$$\varepsilon^*\upsilon^* = \sum\sum\phi_i\phi_j\left(\varepsilon\upsilon\right)_{ij}^*, \qquad \left(\varepsilon\upsilon\right)_{ij}^* = \varepsilon_{ij}^*\upsilon_{ij}^*, \qquad \varepsilon_{ij}^* = \left(\varepsilon_{ii}^*\varepsilon_{jj}^*\right)^{1/2}\left(1 - k_{ij}\right) \tag{6}$$

$$\phi_i = \frac{x_i r_i}{r}, \qquad r = \sum x_i r_i \quad (i = 1, ..., c) \tag{7}$$

The partial derivatives of υ^* and ε^* for the McHugh/Krukonis mixture rules are computed from Equations 8 and 9, respectively [25],

$$\left[\frac{nr}{\upsilon^*}\left(\frac{\partial\upsilon^*}{\partial n_i}\right)_{n_j}\right] = \frac{1}{\upsilon^*}\left[2r_i\left(-\upsilon^* + \sum\phi_j\upsilon_{ij}^*\right)\right] \tag{8}$$

$$\left[\frac{nr}{\varepsilon^*}\left(\frac{\partial\varepsilon^*}{\partial n_i}\right)_{n_j}\right] = \frac{1}{\varepsilon^*\upsilon^*}\left[2r_i\left(-\varepsilon^*\upsilon^* + \sum\phi_j\left(\varepsilon\upsilon\right)_{ij}^*\right)\right] - \left[\frac{nr}{\upsilon^*}\left(\frac{\partial\upsilon^*}{\partial n_i}\right)_{n_j}\right] \tag{9}$$

The SLEOS pure component parameter values obtained from the literature for C3, *trans*-DHN, and *cis*-DHN are shown in Table 1. For computational simplicity, a pseudo-compound comprising 66/34 wt% *trans/cis*-DHN was used. The pseudo-compound pure component parameters were obtained by application of the mixing rules to the two isomers *a priori* in the phase equilibria calculations. In doing this the binary interaction parameters for the two components were assumed to be zero. Ternary phase equilibria calculations for this system entail little added complexity. However, by treating the ternary system (C3, *trans*-DHN, and *cis*-DHN) as a pseudo-binary system (C3 and DHN), a single gas/solvent binary interaction parameter can be used for a gas/solvent/solvent calculation. If the EOS accurately describes the

pseudo-binary gas/solvent PVT behavior, accurate predictions for the polymer solutions are possible by employing the pseudo-binary simplification.

Table 1 Reported SLEOS pure component parameters [12].

Compound	ε^* $(bar\ cm^3/mol)$	v^* (cm^3/mol)	r
C3	30836.1	9.84	6.50
trans-DHN	51630.6	16.37	9.03
cis-DHN	52509.2	15.74	9.15
66/34 wt% *trans/cis*-DHN[a]	51927.2	16.15	9.07

[a] Calculated from pure component values using mixing rules

4. Viscosity model

Tests of the free-volume viscosity model (FVM) developed by Allal et al. [26, 27], derived from a theoretical and physical background, have been reported extensively in the literature. Studies have been reported for both pure fluids [28-32] and for mixtures [33-37]. The FVM is especially useful for describing the behavior of dense fluids (>200 kg/m^3). The model uses the three pure component parameters (ℓ, α and B) to correlate the pure fluid viscosity. The parameter α is characteristic of the barrier energy a molecule must exceed in order for self-diffusion to occur. The characteristic length parameter ℓ accounts for the size of the molecule. The parameter B characterizes the free volume overlap where the free volume in a pure state is defined as the difference between the molar volume and the hard-core volume of the molecule, and arises when the Doolittle theory is incorporated in the derivation of the FVM [27]. With the incorporation of an appropriate dilute gas viscosity model, the FVM can be extended successfully to predict the viscosities of gases, fluids, and their mixtures when densities are less than 200 kg/m^3 [27]. The Allal et al. expression for the viscosity takes the form [27, 28],

$$\eta = \rho \ell \left[\frac{\alpha\rho + (PM/\rho)}{\sqrt{(3RTM)}} \right] \exp\left\{ B \left[\frac{\alpha\rho + (PM/\rho)}{RT} \right]^{3/2} \right\} \tag{10}$$

The characteristic mixture parameters can be calculated using the following mixture rules [29],

$$\alpha_{mix} = \sum_{i=1}^{n} \sum_{j=1}^{n} x_i x_j \alpha_{ij} \qquad \alpha_{ij} = \left(\alpha_i \alpha_j \right)^{1/2} \left(1 - k_{\alpha ij} \right) \tag{11}$$

$$\ell_{mix} = \sum_{i=1}^{n} x_i \ell_i \tag{12}$$

$$\frac{1}{B_{mix}} = \sum_{i=1}^{n} \frac{x_i}{B_i} \tag{13}$$

The binary interaction parameter for viscosity, $k_{\alpha ij}$, was added to the mixture rules to improve the fit of the FVM to experimental data. The binary interaction parameter for viscosity helps to mitigate the detrimental impacts on curve fitting of inaccuracies in the fluid densities needed as inputs to the viscosity model, inaccuracies in pure component viscosity predictions, and/or any shortcomings of the mixing rules used to account for the binary interactions of the fluids.

The FVM pure component parameters for C3, *trans*-DHN and *cis*-DHN obtained from the literature are shown in Table 2. Values of the pure component parameters for a variety of other hydrocarbons, alcohols, refrigerants, carbon dioxide, and water can be found elsewhere [26]. Parameter values for alkoxyethanols [30], polyethers [31], and polyalkylene glycol dimethylethers have also been reported [29, 38].

Table 2 Reported FVM pure component parameters

Compound	$\alpha\ (J\ mol^{-1}m^3kg^{-1})$	$\ell\ (nm)$	$B \times 10^3$
C3 [28]	59.4963	0.0847825	7.392
trans-DHN [29]	100.7	0.09087	10.51
cis-DHN [29]	103.8	0.07493	12.03

5.   Results and discussion

5.1   *Density and phase equilibria*

Tobaly et al. reported spectroscopically measured phase composition data for C3/*cis*-DHN mixtures [38]. We established phase compositions at 392 K for C3 in *cis*-DHN and for C3 in the 66/34 wt% *trans/cis*-DHN for comparison to their data. The good agreement between our view cell measurements and those by Tobaly and coworkers is illustrated in Figure 5. The solubility of C3 is slightly higher in *trans*-DHN than in *cis*-DHN. The *trans* isomer has a lower saturated liquid density when compared to the *cis* isomer. Consequently, *trans*-DHN is expected to have a higher free volume than does *cis*-DHN with concomitantly higher C3 solubility. In addition, the conformational difference between the isomers could impact C3 solubility but there is no rationale for choosing higher C3 solubility in one of the isomers based on conformational preferences. Similar behavior has been observed with the solubility for hydrogen in the two isomers of DHN [39] and we have also observed similar differences with CO_2 solubility in DHN [40]. Nevertheless, based on the experimental findings, the solubility of C3 is expected to be slightly higher in the isomeric mixture than in pure *cis*-DHN.
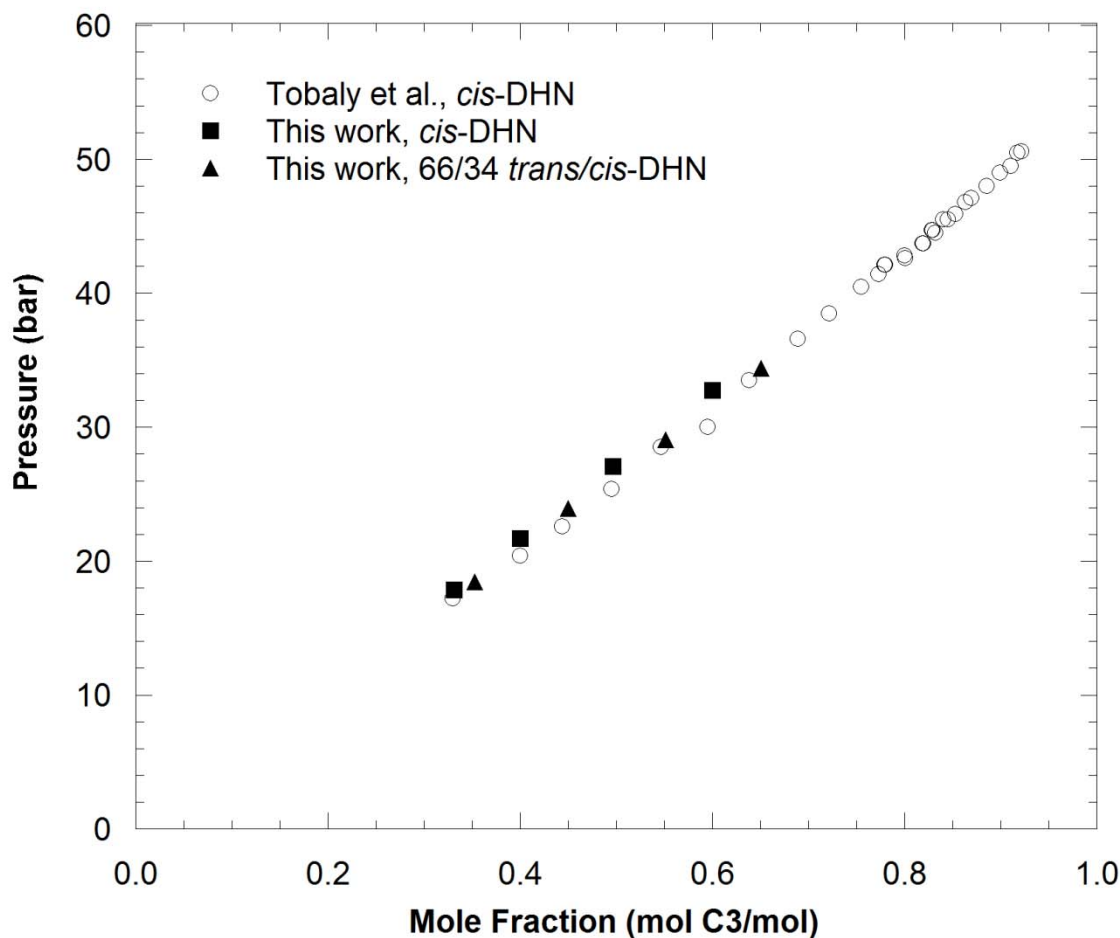
Figure 5 Comparison of measured C3 solubility in *cis*-DHN and 66/34 wt% *trans/cis*-DHN and reported results for C3 in cis-DHN at 392 K

Bubble points for mixtures of C3 (5-65 mol %) in 66/34 wt% *trans/cis*-DHN were measured at 323, 373, and 423 K. The SLEOS was fit to the bubble points using a linearly temperature dependent binary interaction parameter, k_{C3-DHN}, in Equation 6. The value of l_{ij} was set to zero. The P-x plot comparing the experimental data and the curves computed using the SLEOS is shown in Figure 6, which also includes the formula for the temperature dependent binary interaction parameter k_{C3-DHN}. The curves, calculated by using the pseudo-binary mixture approach, clearly give an acceptable fit to the data with an absolute average deviation (AAD) of 5.3%. The experimental uncertainty for the bubble point measurements was 3.5%. We also

fitted the data using a three-component model. Since deconvoluting the *cis*-DHN/C3, *trans*-DHN/C3, and *cis*-DHN/*trans*-DHN pair-wise interactions was problematic, we assumed the C3/DHN binary interaction parameters were equal ($k_{C3\text{-}cisDHN} = k_{C3\text{-}transDHN}$) for the three-component calculation. No significant difference between the three-component and two-component pseudo-binary fit to the bubble points was found.

The single binary interaction parameter $k_{C3\text{-DHN}}$ was calculated for the pseudo-binary mixture of C3 in a pseudo-component comprising 66/34 wt% *trans/cis*-DHN. While this parameter is specific to the 66/34 wt% mixture of *trans/cis* isomers and does not necessarily apply to other pseudo-component ratios, our ability to fit P-x for both *cis*-DHN and the 66/34 pseudo-binary mixture suggests that the value of $k_{C3\text{-DHN}}$ obtained can be used with good results for other *trans/cis* combinations.
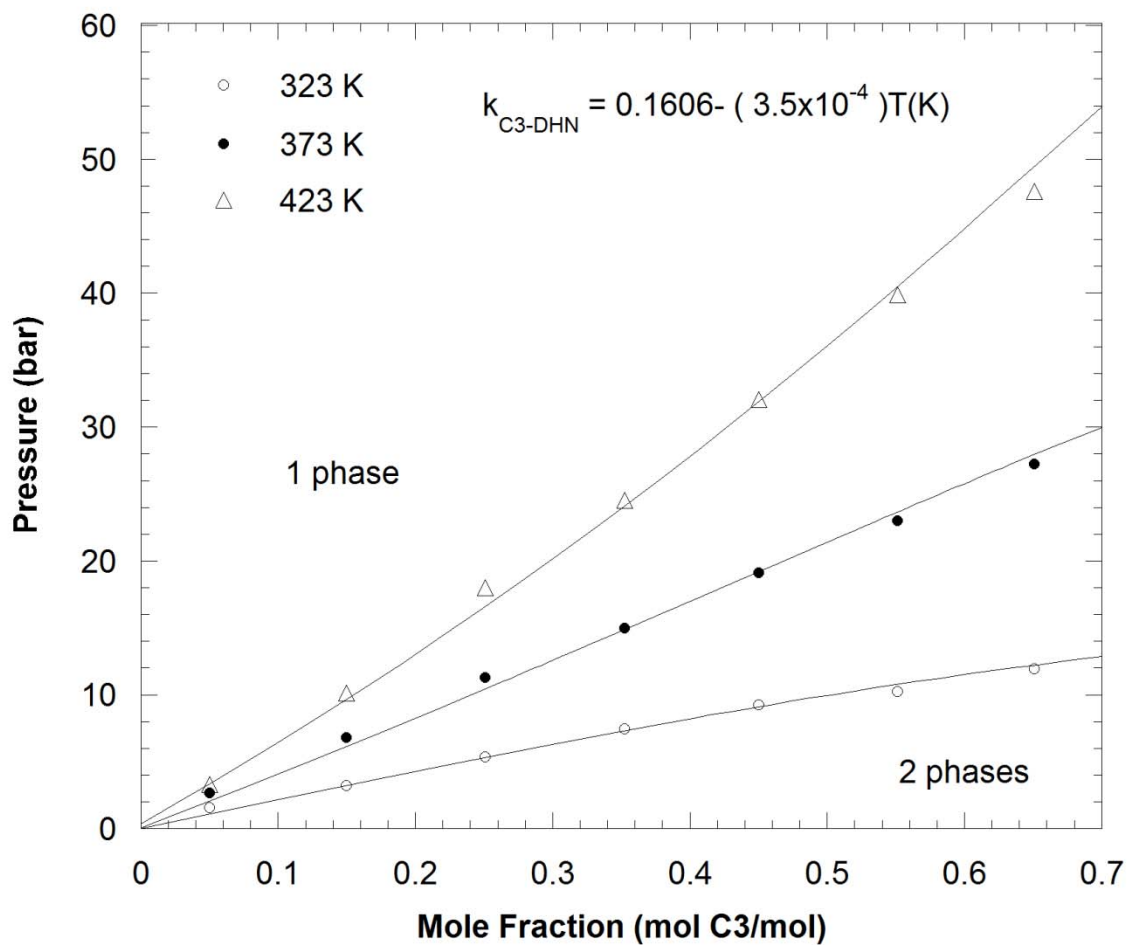
Figure 6   C3 solubility in pseudo DHN (66/34 wt% *trans/cis*-DHN) from this work; solid

lines pseudo-binary SLEOS results

Table 3 Tabulated data for C3 solubility in 66/34 wt% *trans/cis*-DHN

x_{C3} (mol C3/mol)	P_{BP} (bar), 323 K	P_{BP} (bar), 373 K	P_{BP} (bar), 423 K
0.05	2	3	3
0.15	3	7	10
0.25	5	11	18
0.35	7	15	25
0.45	9	19	32
0.55	10	23	40
0.65	12	27	48

Miyake and coworkers investigated the influence of stereoisomers of DHN on PVT

properties using a vibrating-tube densimeter [41]. Miyake and coworkers tested three density

models against their data for pure *trans*-DHN, *cis*-DHN, and their mixtures. The Peng-Robinson equation-of-state (PREOS), the perturbed chain-statistical associating fluid theory (PC-SAFT), and the molecular dynamics (MD) approach by Miyake et al. yielded similar absolute average deviations of less than 1% for 294 points at 7 different compositions, including the two neat isomers, three temperatures of 303.15, 323, and 343.15 K, and 14 different isobars over the range 1-to-650 bars.

We have compared SLEOS predictions to the entire data set of Miyake et al. and their data and the predictions at 1 bar and 650 bars in Figure 7. For the set of 294 data points, the AAD obtained using the SLEOS was 0.38%. The SLEOS compressed liquid density predictions for the pure isomers *trans*-DHN and *cis*-DHN and the *trans/cis*-DHN mixtures capture the data qualitatively, but the biased error (0.24%) is larger than the experimental error (~0.06%) reported by the authors. Even though the error between the model and their data is on the order of ten times more than the authors' experimental error, the model predictions compared to their data are still more than adequate for engineering design work. Indeed, the SLEOS predictions to their data are better than the three models tested by the authors.
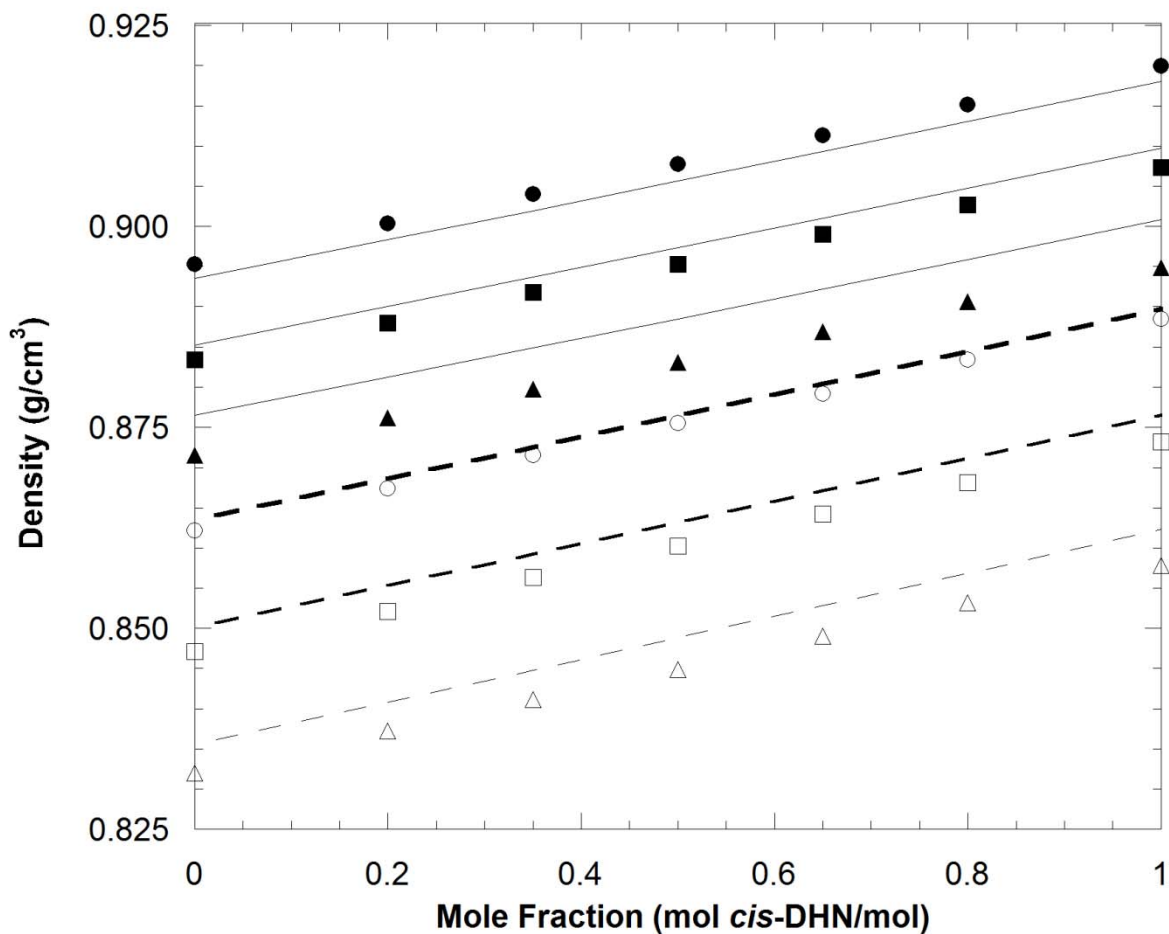
Figure 7   SLEOS density calculations from this work for DHN mixtures, data from Miyake et al. [41] (unfilled triangles-1 bar, 343.15 K, unfilled squares-1 bar, 323 K, unfilled circles-1 bar, 303.15 K, filled triangles-600 bar, 343.15K, filled squares-600 bar, 323 K, filled circles-600 bar, 303.15 K)

The saturated liquid densities of the pseudo-binary mixtures of C3 in 66/34 wt% *trans/cis*-DHN were measured at the bubble point of each mixture at 323K, 373 K, and 423 K. In Figure 8, densities computed using the SLEOS are compared to the experimental solution densities. There does appear to be some systemic bias for the density predictions but the AAD was 0.92% and the experimental uncertainty was estimated as 0.83%.
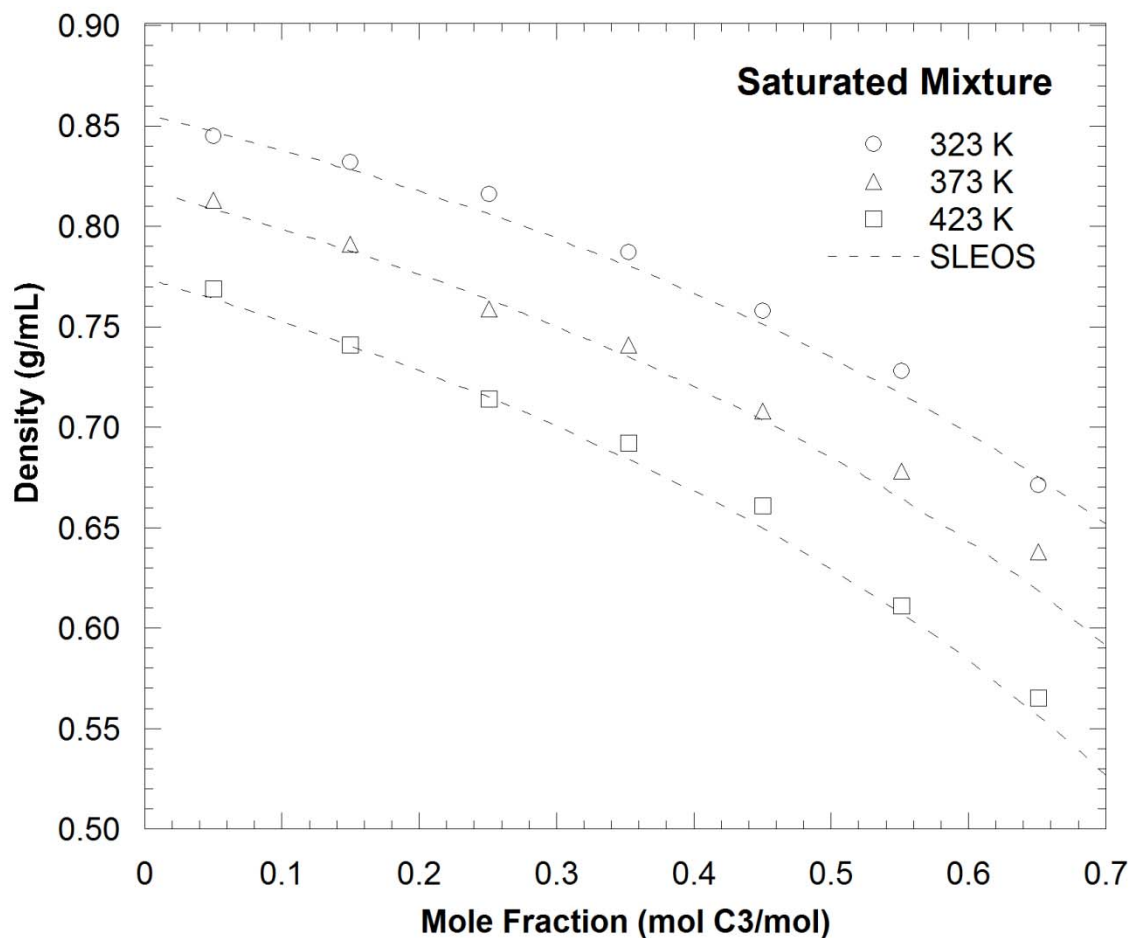
Figure 8 Saturated liquid density of C3 in 66/34 wt% *trans/cis*-DHN mixtures vs. C3 concentration and SLEOS calculation results from this work

Table 4 Tabulated data for saturated liquid density of C3 in 66/34 wt% *trans/cis*-DHN mixtures

x_{C3} (mol C3/mol)	ρ^{SL} (g/mL), 323 K	ρ^{SL} (g/mL), 373 K	ρ^{SL} (g/mL), 423 K
0.05	0.845	0.813	0.769
0.15	0.832	0.791	0.741
0.25	0.816	0.759	0.714
0.35	0.787	0.741	0.692
0.45	0.758	0.708	0.661
0.55	0.728	0.678	0.611
0.65	0.671	0.638	0.565

To better understand the volume expansion (VE) behavior of C3/DHN mixtures, Equation 14 is used to calculate the VE, defined as the specific volume of the C3/DHN mixture,

V^{MIX}, at a given temperature and pressure divided by the specific volume of the DHN mixture, V^{DHN}, at the same temperature and pressure,

$$VE = \frac{V^{MIX}(T,P)}{V^{DHN}(T,P)} \qquad (14)$$

The results for the VE of the saturated liquid and the compressed fluid at one isotherm are shown in Figure 9.

Two other VE-P isotherms were measured (323 K and 423 K) and similar behavior was observed. The maximum VE measured of 1.385 occurs at 423 K and at the bubble point for a mixture of 65% C3 in DHN. The SLEOS predictions for the single-phase mixture densities capture the qualitative behavior of the data reasonably well with an absolute average deviation of 2.3% for 63 data points.

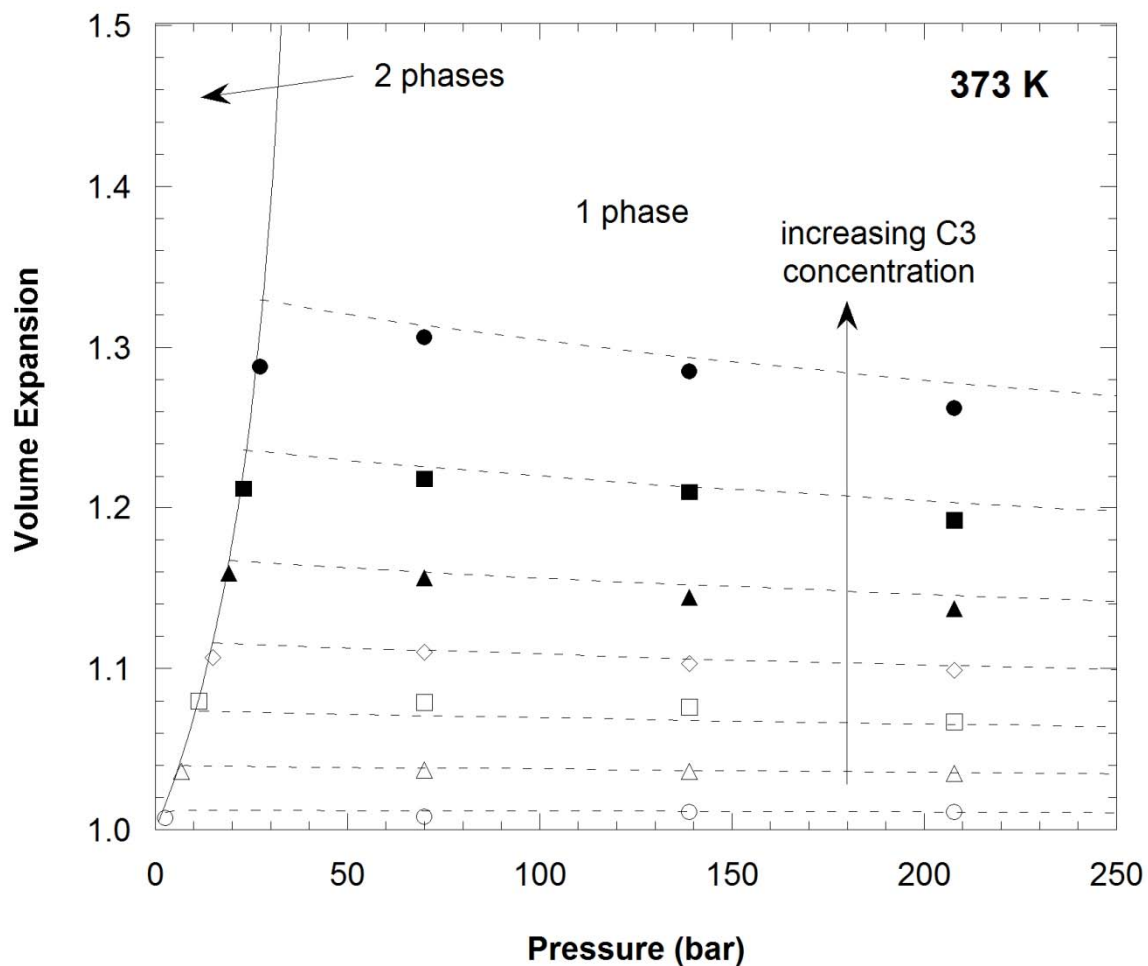**Figure 9**   VE-P projection from this work for pseudo-binary propane in 66/34 wt% *trans/cis*-DHN mixture at 373 K (filled circles-65 mol% C3, filled squares-55 mol% C3, filled triangles-45 mol% C3, unfilled diamonds-35 mol% C3, unfilled squares-25 mol% C3, unfilled triangles-15 mol% C3, unfilled circles-5 mol% C3)

Table 5 Tabulated data for volume expansion of C3 in 66/34 wt% *trans/cis*-DHN mixtures

T (K)	x_{C_3} (mol C3/mol)	VE, P_{sp}	VE, 70 bar	VE, 139 bar	VE, 208 bar
323	0.05	1.014	1.010	1.012	1.010
	0.15	1.030	1.032	1.032	1.023
	0.25	1.050	1.060	1.064	1.056
	0.35	1.089	1.084	1.093	1.080
	0.45	1.131	1.124	1.126	1.122
	0.55	1.178	1.169	1.170	1.173
	0.65	1.277	1.246	1.235	1.233
373	0.05	1.007	1.008	1.011	1.011
	0.15	1.036	1.037	1.036	1.035
	0.25	1.080	1.079	1.076	1.067
	0.35	1.107	1.110	1.103	1.099
	0.45	1.159	1.156	1.144	1.137
	0.55	1.212	1.218	1.210	1.192
	0.65	1.288	1.306	1.285	1.262
423	0.05	1.007	1.017	1.018	1.007
	0.15	1.047	1.045	1.041	1.034
	0.25	1.089	1.081	1.078	1.074
	0.35	1.125	1.125	1.117	1.109
	0.45	1.179	1.193	1.180	1.165
	0.55	1.278	1.258	1.248	1.226
	0.65	1.385	1.386	1.327	1.314

The saturated liquid curve on the VE-P isotherm (solid line) shows an increase in the volume expansion (VE) with pressure. As the system pressure is raised for a two-phase system, more C3 is dissolved in the liquid resulting in an increase in the VE of the liquid phase. The single-phase VE (dashed curve) is relatively insensitive to an increase in pressure over the range of pressures measured. Even though the mixture density decreases with increasing C3 concentration (i.e. the fluid is less liquid-like), the single phase mixture is relatively incompressible. This phenomenon is advantageous at the high pressures required to obtain moderately high polymer concentrations. At these conditions, the expanded fluid phase will exhibit low viscosities and enhanced rates of mass transfer without sacrificing the high polymer concentrations needed to obtain a highly productive hydrogenation process.

5.2   *Viscosity*

Zéberg-Mikkelsen and coworkers reported the viscosities of pure isomers of DHN over a wide range of pressures and temperatures [28]. Having obtained three pure component parameters for both the *cis* and the *trans*-DHN, the authors rationalized the differences in the parameter sets using differences in the molecular configurations of the isomers. The same structural features that make the *cis* isomer a higher density fluid were cited as the dominating factor leading to significantly higher values of the free volume overlap and lower values of the characteristic length.

The differences between saturated liquid viscosities of the pure DHN isomers and our FVM predictions for viscosity are shown in Figure 10. The 66/34 wt% *trans/cis*-DHN saturated liquid mixture viscosity is also shown for comparison. The model results shown in Figure 10 were computed using the parameter values reported by Zéberg-Mikkelsen et al. The agreement between the FVM predictions for the pure isomers and the isomeric mixture of DHN is excellent with an AAD of 2.3%, consistent with the AADs reported by Zéberg-Mikkelsen.
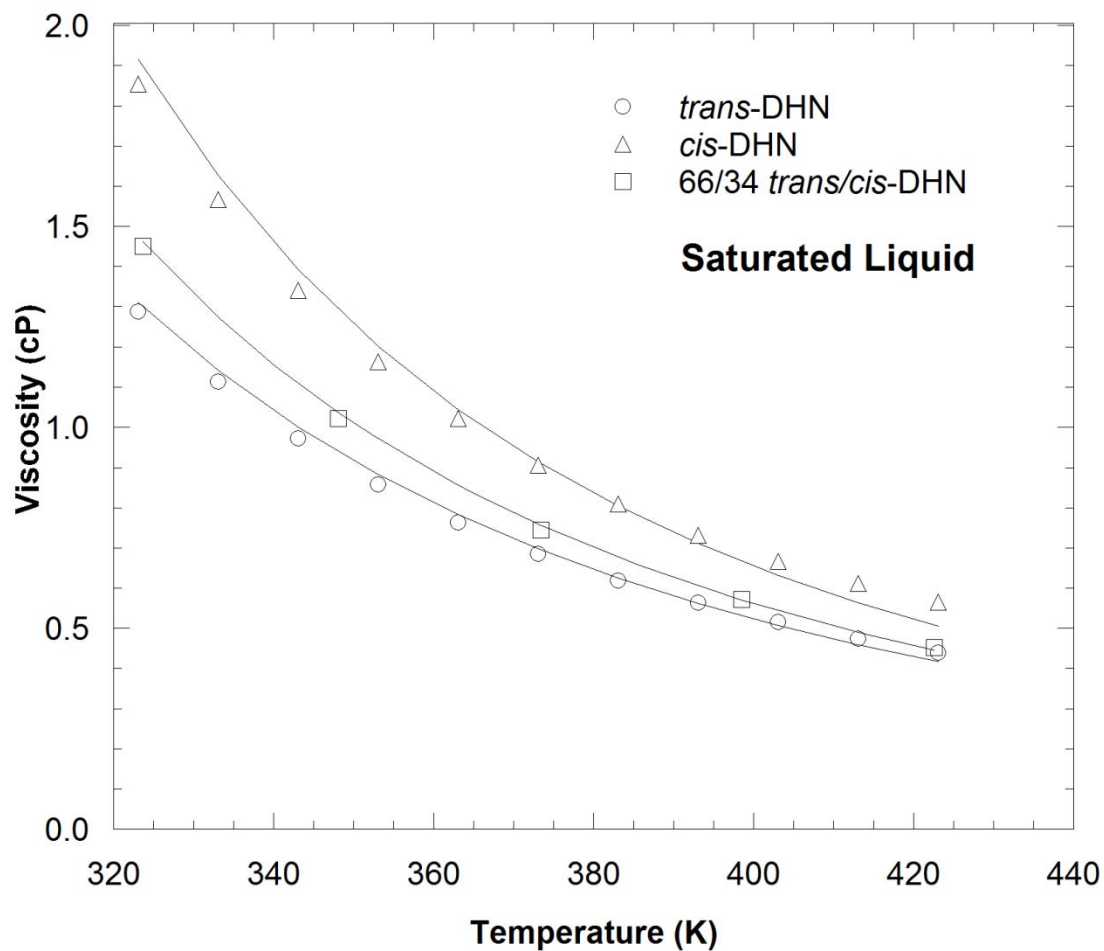
Figure 10 Measured saturated liquid viscosity of pure isomers of DHN and a 66/34 *trans*/*cis*-DHN mixture from this work, Curves are FVM predictions using SLEOS for density predictions

Table 6 Tabulated data for saturated liquid viscosity of isomers of DHN and 66/34 wt% *trans/cis*-DHN mixture

T (K)	η_{trans} (cP)	η_{cis} (cP)	T (K)	$\eta_{trans/cis}$ (cP)
323	1.29	1.86	324	1.45
333	1.11	1.57	348	1.02
343	0.97	1.34	373	0.75
353	0.86	1.16	399	0.57
363	0.76	1.02	423	0.45
373	0.68	0.91		
383	0.62	0.81		
393	0.56	0.73		
403	0.52	0.67		
413	0.47	0.61		
423	0.44	0.56		

Isobaric C3/DHN compressed liquid mixture viscosity data at 139 bar for six C3 concentrations at five temperatures are shown in Figure 11. Similar measurements were made at 70 bar, 208 bar, and at the bubble point pressure of the mixture. The FVM was fit to the C3/DHN mixture viscosity data for all three isobars by varying the viscosity binary interaction parameter, $k_{\alpha C3\text{-}DHN}$, as shown in Equation 12. When the binary interaction parameter was not used, the model captured the data well qualitatively, but the AAD was 14.5% with a bias of 13.5%. When a best-fit binary interaction parameter ($k_{C3\text{-}DHN}$ = -0.199) was used, a considerably better fit to the data was obtained (AAD of 5.7% and bias of 0.29%).
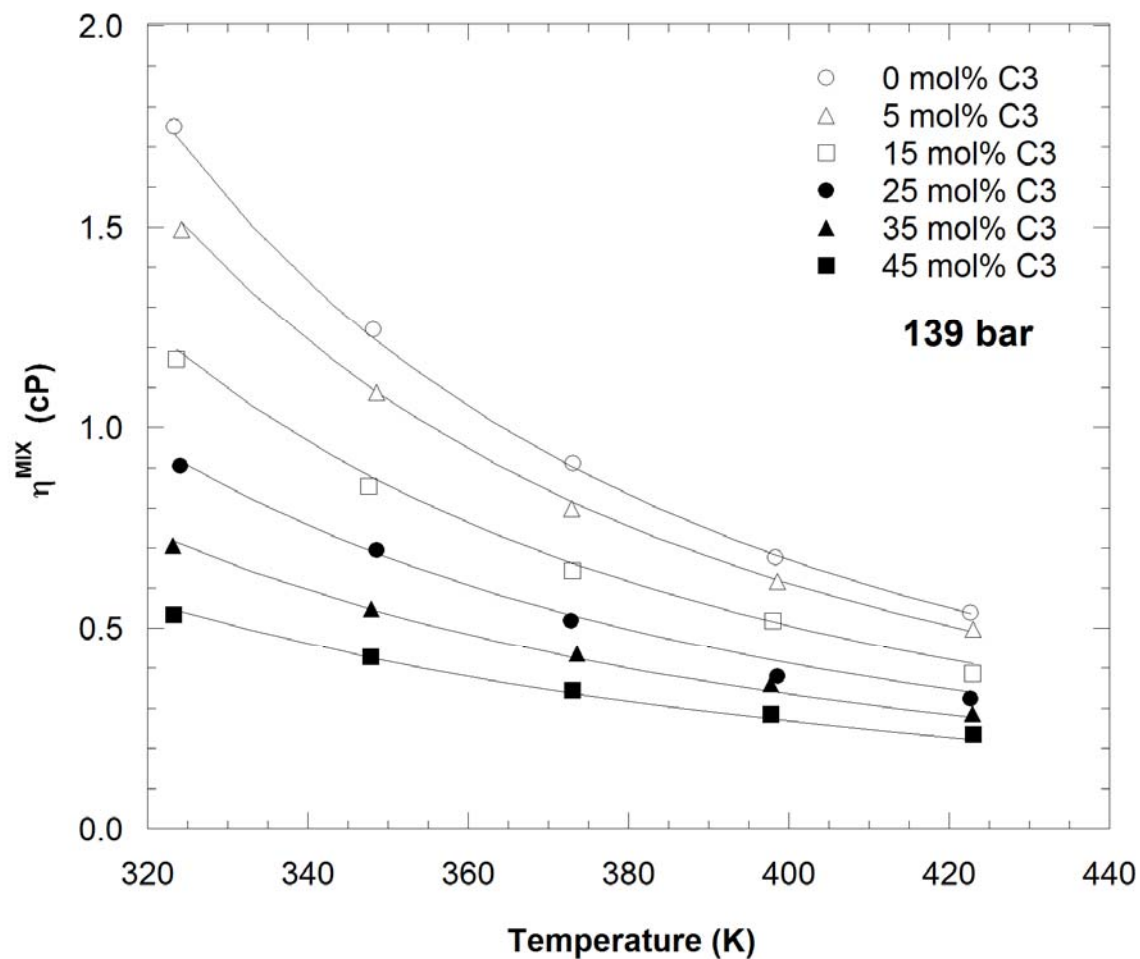
Figure 11 Measured viscosity of C3 in 66/34 *trans/cis*-DHN at 139 bar from this work,

Curves are FVM predictions with SLEOS density predictions [k_{C3-DHN} = -0.199]

Table 7 Tabulated viscosity data for C3 in 66/34 wt% *trans/cis*-DHN mixtures

	0 mol% C3		5 mol% C3		15 mol% C3		25 mol % C3		35 mol% C3		45 mol% C3	
P (bar)	T (K)	η (cP)	T (K)	η (cP)	T (K)	η (cP)	T (K)	η (cP)	T (K)	η (cP)	T (K)	η (cP)
70	324	1.60	325	1.38	324	1.05	324	0.85	323	0.67	323	0.50
	348	1.14	349	0.97	348	0.78	349	0.64	348	0.51	348	0.40
	373	0.83	373	0.73	373	0.58	373	0.47	373	0.40	373	0.32
	398	0.63	399	0.57	398	0.48	399	0.35	398	0.33	398	0.26
	423	0.49	423	0.46	423	0.35	423	0.28	423	0.25	423	0.22
139	323	1.75	324	1.49	324	1.17	324	0.90	323	0.71	323	0.53
	348	1.25	349	1.09	348	0.85	349	0.69	348	0.55	348	0.43
	373	0.91	373	0.80	373	0.64	373	0.52	374	0.43	373	0.34
	398	0.68	399	0.62	398	0.52	399	0.38	398	0.36	398	0.28
	423	0.54	423	0.50	423	0.39	423	0.32	423	0.29	423	0.23
208	50	1.85	324	1.61	324	1.24	324	0.96	323	0.75	323	0.58
	75	1.33	348	1.19	348	0.91	348	0.74	348	0.58	348	0.46
	100	0.99	372	0.86	373	0.69	373	0.58	373	0.47	373	0.37
	124	0.75	399	0.66	398	0.56	398	0.42	398	0.39	399	0.31
	149	0.59	423	0.54	423	0.45	423	0.36	423	0.30	423	0.25

The influence of C3 on the mixture viscosity can be evaluated with the viscosity reduction (VR) as defined by the expression,

$$VR = 1 - \frac{\eta^{MIX}(T,P)}{\eta^{DHN}(T,P)}$$ (15)

One VR-P isotherm at 373 K is shown in Figure 12. The liquid mixture viscosity measurements taken on the two phase system exhibited similar behavior to the VE-P isotherms. The VR for the single-phase concentration isopleths is mostly insensitive to an increase in pressure over the entire range of the data, as was similarly observed in the volume expansion behavior. The highest VR occurs at the highest C3 concentration measured (45 mol% C3) and the highest temperature (423 K).
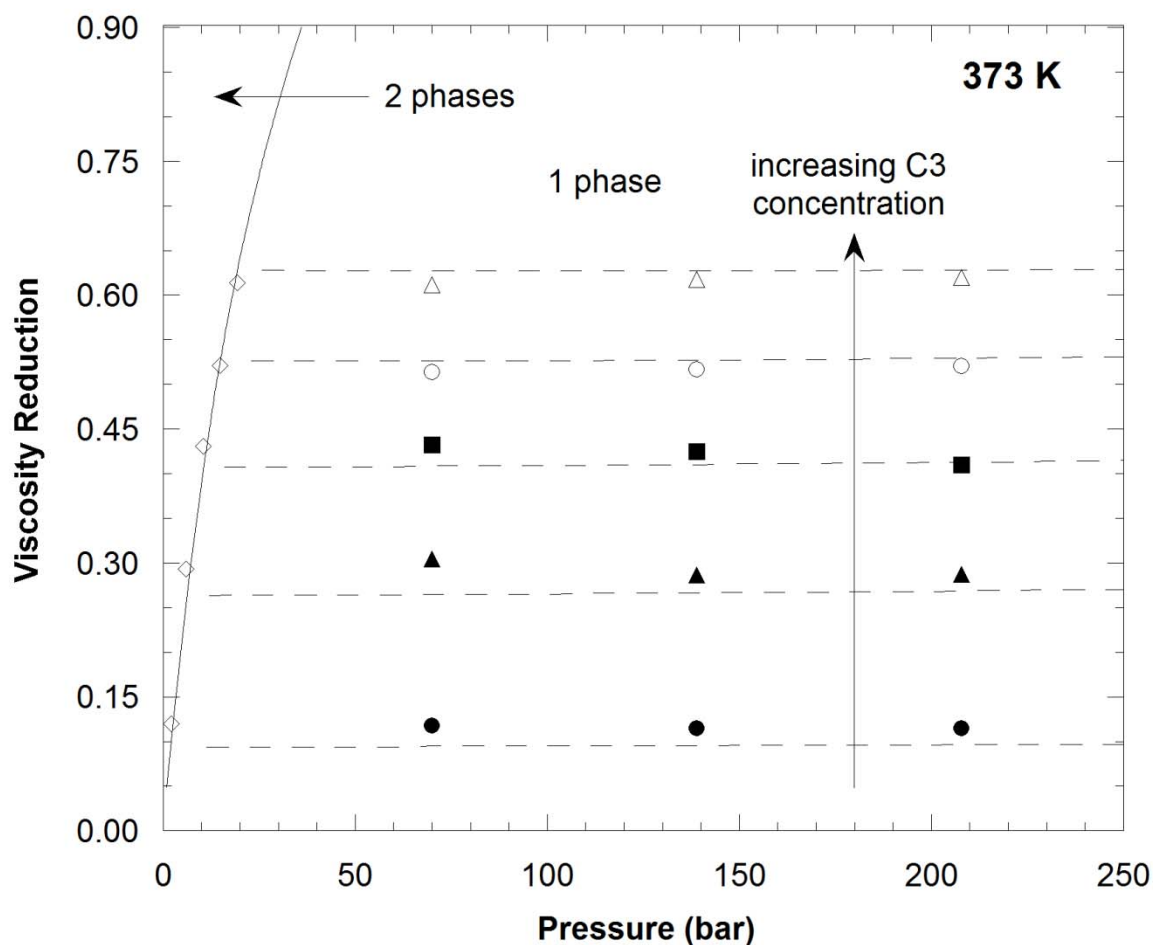
Figure 12   VR-P projection from this work for mixtures of C3 in 66/34 *trans*/*cis*-DHN at 373 K (unfilled diamonds-saturated liquid, unfilled triangles-45 mol% C3, unfilled circles-35mol% C3, filled squares-25 mol% C3, filled triangles-15 mol% C3, filled circles-5 mol% C3)

5.3   *Correlation of viscosity reduction to volume expansion*

The magnitude of viscosity reduction of DHN by C3 at various temperatures and pressures is almost entirely dependent on the volume expansion of DHN by C3. We've plotted the viscosity reduction (necessarily a normalized viscosity value) versus the volume expansion (specific volume of the mixture relative to pure DHN) in Figure 13. The specific volume of the mixture captures variations in temperature, pressure, and dilution thus Figure 13 correlates the viscosity reduction to the complete physical state of the fluid.

The collapse of the data onto a single curve is incomplete, suggesting that other physical attributes of the mixture also influence the viscosity reduction. However, the degree of separation of the data from a single curve is relatively small therefore much of the viscosity reduction can be attributed to the expansion of the fluid phase by C3.
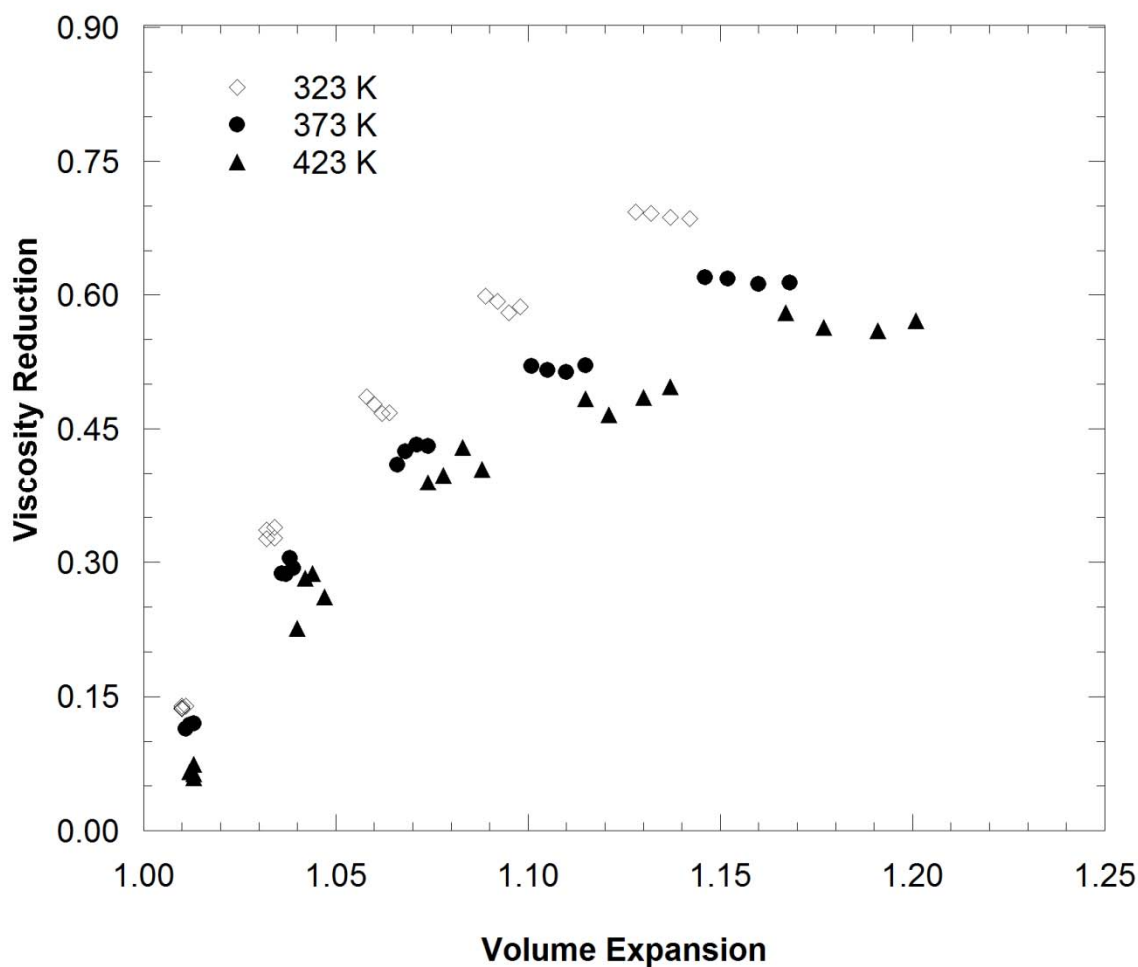

Figure 13   VR vs. VE from this work for mixtures of C3 in 66/34 *trans/cis*-DHN

6.   Conclusions

A range of temperatures, pressures and compositions of C3/DHN mixtures suitable for solvation of polystyrene has been investigated by means of phase equilibria, density, and viscosity measurements. Phase equilibria and density data of the pure components and mixtures were captured quite well by the SLEOS. The SLEOS calculations were used to feed biphasic

and single fluid densities to the FVM for calculating pure component viscosities and viscosities of the mixtures. The calculations lead to very good agreement between the FVM for viscosity and the data with a single adjustable parameter. Even though a binary interaction parameter for viscosity was required to obtain a good fit to the data the calculations can still provide utility for future calculations that require interpolated data that is both complex and laborious.

List of symbols

B   characteristic of the free volume overlap (FVM)

c   total number of components in the mixture

k   fitted mixture parameter accounting for specific binary interactions between components in the mixture (SLEOS and subscript α indicating for FVM)

l   fitted mixture parameter roughly accounting for free volume differences between components in the mixture (SLEOS, not used in this work)

M   molecular weight

n   moles

P   pressure

r   number of lattice sites per molecule (SLEOS)

R   universal gas constant

T   temperature

V   specific volume

x   mole fraction

z   compressibility factor

Greek symbols

α characteristic barrier energy a molecule must overcome for self-diffusion to occur (FVM)

ε interaction energy per mer (SLEOS)

ϕ close-packed volume fraction in the mixture at the incompressible state (SLEOS)

φ fugacity coefficient

η dynamic viscosity

ρ mass density

υ SLEOS hard-core molecular volume (SLEOS)

ℓ characteristic molecular length parameter (FVM)

Subscripts/superscripts

α indicating binary interaction parameter, k , is for FVM

i, j   for compound i, j, etc.

*   characteristic variable

~   reduced variable

MIX   mixture variable

DHN   76/24 wt% *trans/cis*-decahydronaphthalene variable

C3   propane variable

Abreviations

VE   volume expansion

VR   viscosity reduction

C3   propane

DHN   decahydronaphthalene (assumed 76/24 wt% *trans/cis* unless otherwise stated by *t* or *c*

indicating the *trans* or *cis* isomer, respectively)

References

1. M. Wei, , G.T. Musie, ,D.H. Busch, B. Subramaniam, *J. Am. Chem. Soc.*, 124 (2002) 2513-2517.

2. B. Rajagopalan, B. Subramaniam, D.H. Busch, *Ind. Eng. Chem. Res.*, 42 (2003) 6505-6510.

3. B. Kerler, A.S. Robinson, B. Subramaniam, *App. Catal. B: Env.*, 49 (2004) 91-98.

4. D. Xu, R.G. Carbonell, D.J. Kiserow, G.W. Roberts, *Ind. Eng. Chem. Res.*, 44 (2005) 6164-6170.

5. G.W. Roberts, D. Xu, D.J. Kiserow, R.G. Carbonell, Hydrogenation of Polymers in the Presence of Supercritical Carbon Dioxide. U.S. Patent Application No.: US 2007/0270554 A1

6. D. Chouchi, D. Gourgouillon, M. Courel, J. Vital, M. Nunes da Ponte, *Ind. Eng. Chem. Res.*, 40 (2001) 2551-2554.

7. L.B. Dong, PhD thesis, Department of Chemical Engineering, North Carolina State University (2010)

8. C.A. Irani, C. Cozewith, S.S. Kasegrande, Method for High Temperature Phase Separation of solutions Containing Ethylene Copolymer Elastomers, U.S. Pat. 4,319,021, (1982).

9. M.A. McHugh, T.L. Guckes, *Macromolecules*, 18 (1985) 674-680.

10. A.J. Seckner, A.K. McClellan, M.A. McHugh, *AIChE Journal*, 34 (1988) 9-16.

11. E. Kiran, W. Zhuang, Y.L. Sen, *J. Appl. Polym. Sci.*, 47 (1993) 895-909.

12. B. Bungert, G. Sadowski, W. Arlt, *Fluid Phase Equilib.*, 139 (1997) 349-359.

13. N. Koak, T.W. de Loos, R.A. Heidemann, *Fluid Phase Equilib.*, 145 (1998) 311-323.

14. I. Nagy, T.W. de Loos, R.A. Krenz, R.A. Heidemann, *J. Supercrit. Fluids*, 37 (2006) 115-124.

15. *The Merck Index: An Encyclopedia of Chemicals, Drugs, and Biologicals*, Fourteenth Edition, Maryadele J. O'Neil, Patricia E. Heckelman, Cherie B. Koch, Kristin J. Roman, Eds. (Merck & Co., Inc., Whitehouse Station, NJ, USA, 2006).

16. S. Jiang, L. An, B. Jiang, B.A. Wolf, *Chemical Physics*, 298 (2004) 37-45.

17. W.M. Haynes, R.D. Goodwin, National Bureau of Standards Monograph 170, Boulder, Colorado (1982).

18. B.A. Younglove, J.F. Ely, *J. Phys. Chem. Ref. Data*, 16, (1987) 577-798.

19. I.C. Sanchez, R.H. Lacombe, *Nature*, 252 (1974) 381-383.

20. I.C. Sanchez, R.H. Lacombe, *J. Phys. Chem.*, 80 (1976) 2352-2362.

21. I.C. Sanchez, R.H. Lacombe, *Macromolecules*, 11 (1978) 1145-1156.

22. E. Neau, *Fluid Phase Equilib.*, 203 (2002) 133-140.

23. C.A. Mertdogan, H. Byun, M.A. McHugh, W.H. Tuminello, *Macromolecules*, 29 (1996) 6548-6555.

24. Y. Xiong, E. Kiran, *Polymer*, 35 (1994) 4408-4415.

25. M.A. McHugh, V.J. Krukonis, Supercritical Fluid Extraction: Principles and Practice, 2nd Edition, H. Brenner, Boston (1993).

26. A. Allal, M. Moha-Ouchane, C. Boned, *Phys. Chem. Liq.*, 39 (2001) 1-30.

27. A. Allal, C. Boned, A. Baylaucq, *Phys. Rev. E.*, 64 (2001) 011203-1-011203-10.

28. C.K. Zéberg-Mikkelsen, A. Baylaucq, M. Barrouhou, C. Boned, *Phys. Chem. Chem. Phys.*, 5 (2003) 1547-1551.

29. M.J.P. Comuñas, A. Baylaucq, F. Plantier, C. Boned, J. Fernández, *Fluid Phase Equilib.*, 222-223 (2004) 331-338.

30. P. Reghem, A. Baylaucq, M.J.P. Comuñas, J. Fernández, C. Boned, *Fluid Phase Equilib.*, 236 (2005) 229-236.

31. A. Baylaucq, M.J.P. Comuñas, C. Boned, A. Allal, J. Fernández, J., *Fluid Phase Equilib.*, 199 (2002) 249-263.

32. C. Boned, C.K. Zéberg-Mikkelsen, A. Baylaucq, P. Daugé, *Fluid Phase Equilib.*, 212 (2003) 143-164.

33. M.A. Monsalvo, A. Baylaucq, P. Reghem, S.E. Quiñones-Cisneros, C. Boned, *Fluid Phase Equilib.*, 233 (2005) 1-8.

34. A. Baylaucq, C. Boned, X. Canet, C.K. Zéberg-Mikkelsen, S.E. Qiñones-Cisneros, H Zhou, *Petroleum Science and Technology*, 23 (2005) 143-157.

35. X. Canet, P. Daugé, A. Baylaucq, C. Boned, C.K. Zéberg-Mikkelsen, S.E. Qiñones-Cisneros, E.H. Stenby, *Int. J. Thermophys.*, 22 (2001) 1669-1689.

36. C.K. Zéberg-Mikkelsen, G. Watson, A. Baylaucq, G. Galliéro, C. Boned, *Fluid Phase Equilib.*, 245 (2006) 6-19.

37. A. Baylaucq, C. Boned, X. Canet, C.K. Zéberg-Mikkelsen, *Int. J. Thermophys.*, 24 (2003) 621-637.

38. P. Tobaly, P. Marteau, V. Ruffier-Meray, J. Chem. Eng. Data, 49 (2004) 795-799.

39. T. Tsuhi, K. Sue, T. Hiaki, N. Itoh, *Fluid Phase Equilib.,* 257 (2007) 183-189.

40. N. Cain, R. Carbonell, D. Kiserow, G. Roberts, 5th International Symposium in Chemical Engineering and High Pressure Processes, Segovia, Spain (2007).

41.   Y. Miyake, A Baylaucq, C.K. Zéberg-Mikkelsen, G. Galliéro, H. Ushiki, C. Boned, *Fluid Phase Equilib*., 252 (2007) 79-87.